Hindawi
Mathematical Problems in Engineering
Volume 2020, Article ID 3054969, 11 pages
https://doi.org/10.1155/2020/3054969

Research Article

Modeling of Marine Asynchronous Shaft Generator and Simulation of Subsynchronization State

Yan Langtao, Tan Jiawan, Liu Yusheng, and Yang Hui

School of Shipping and Naval Architecture, Chongqing Jiaotong University, Chongqing 400074, China

Correspondence should be addressed to Tan Jiawan; 6181141@qq.com

Received 16 August 2020; Revised 29 September 2020; Accepted 15 October 2020; Published 3 November 2020

Academic Editor: William Guo

The new type of marine asynchronous shaft generator has the advantages of adjustable excitation and power factor, compared to the traditional synchronous shaft generator, and has been widely used. However, the traditional synchronous shaft generator simulation system is still used in domestic ship power station simulators, which seriously restricts the renewal of crew training. In order to overcome the shortage of the simulation system of doubly fed shaft generator for ship power plant simulator, in this paper, the mathematical model of marine doubly fed shaft system is established for the first time, according to the characteristics of doubly fed machine and marine shaft generator. This paper realizes power decoupling by stator flux orientation and simulates and analyses the asynchronous shaft generator under subsynchronous working conditions. The changing trend of each physical quantity in the simulation waveform meets the mathematical relationships of the actual physical quantity, which proves the correctness of the mathematical model and lays a theoretical foundation for the development of the simulation system of asynchronous shaft generator.

1. Introduction

The marine asynchronous shaft generator is different from the traditional synchronous shaft generator. It has many remarkable characteristics, but the traditional synchronous shaft generator has no such characteristics. These remarkable characteristics include adjustable power factor, a wide range of speed variation, and small converter-capacity. The capacity of the converter is only slip power. It is suitable for the variable speed and constant frequency power generation system, such as the speed of the main engine of the ship, which frequently changes due to the complex and changeable sea conditions. Therefore, the asynchronous generator is more suitable for the marine shaft generator than the synchronous generator. The stator of the marine asynchronous shaft generator is connected to the marine power grid, and the rotor winding usually provides a three-phase low-frequency excitation current with adjustable amplitude, frequency, phase sequence, and phase through the dual PWM converter [1].

The marine asynchronous shaft generator is a new type of marine shaft generator, which has the function of energy saving and environmental protection and will gradually replace the traditional synchronous shaft generator. It will promote the renewal of the marine shaft generator system and gradually occupy the leading position of the marine shaft generator system. However, the renewal of marine mechanical and electrical equipment will bring the challenge of knowledge renewal and operation skill renewal to the marine engineers or electrical engineers. It is also a great difficulty to improve the management level and operation experience of the management of the marine asynchronous shaft generator system in a short time. The effective method is to use a ship power station simulator to train them without operating the real ship.

But at present, there is no marine asynchronous shaft generator system in the marine power plant simulator. The present situation makes the crew's training on the marine asynchronous shaft generator only conducted on the basis of synchronous shaft generator in the form of oral, without real operation on the marine asynchronous shaft generator. It

makes the updating of crew operation technology far behind the updating of existing electromechanical equipment. The building of the marine asynchronous shaft generator simulation system is of great significance to promote the development of ship electronic and electrical technology and even the development of the shipping business.

The necessary prerequisite for the development of the marine asynchronous shaft generator simulation system is the correct mathematical modeling of the system. The correctness and validity of the mathematical model are very important because only the correct and complete mathematical model can accurately reflect the typical characteristics and real-time dynamic process of the ship's shaft generator system [2, 3].

2. Mathematical Model

2.1. The Structure Diagram of the Marine Asynchronous Shaft Generator. According to the working principle of marine main engine and shaft generator, the structure diagram of the marine asynchronous shaft generator system is designed, as shown in Figure 1. The system uses the surplus power of the main engine driving the propeller to drive the asynchronous generator to generate electricity. The rotating speed on the main engine shaft of the ship will change with the sea state and waterway, which caused the rotor speed (represented by the letter n as shown in Figure 1) of the asynchronous generator to accordingly be changed. Therefore, the marine asynchronous shaft generator may work in different working states, such as subsynchronization, synchronization, and supersynchronization.

In order to ensure that the frequency of the stator output voltage of the marine asynchronous shaft generator is constant under different working conditions, the system adopts the dual PWM converter to realize AC excitation. The dual PWM converter rectifies the AC of the marine power grid into DC, and then inverts it into suitable AC with a certain amplitude, a certain frequency, and a certain phase, and sends it to the rotor of the marine asynchronous shaft generator for excitation.

It is assumed that the rotor winding and stator winding are symmetrical, and the number of pole pairs is p. When the voltage of frequency f_1 coming from the ship power grid is applied to the stator of the asynchronous generator, the stator winding will flow through the three-phase symmetrical alternating current, which creates a rotating magnetic field on the stator. The rotating speed of the rotating magnetic field is expressed as letter n_1. The relationship between the rotation speed of the rotating magnetic field and the pole number (expressed as letter p) can be shown as in the following formula:

$$n_1 = \frac{60 f_1}{p}. \tag{1}$$

Similarly, when the excitation current of the rotor with a certain frequency (expressed as letter f_2) is applied to the three-phase symmetrical rotor winding, a rotating magnetic field relative to the rotor itself will be generated. The corresponding speed and frequency are expressed as n_2 and f_2, respectively, which also meets the expression shown as formula (1).

It can be seen from formula (1) that the frequency (expressed as letter f_2) of excitation current coming from rotor determines the speed (expressed as letter n_2) of the corresponding magnetic field rotation [4], and the phase sequence of the excitation current determines the rotation direction of the corresponding magnetic field [5].

When the frequency of the ship power grid is 50 Hz, the speed of the stator rotating magnetic field of the marine asynchronous shaft generator is expressed by the letter n_1. To ensure that the frequency (expressed as letter f_1) of stator voltage of the marine asynchronous shaft generator is constant under different rotor speeds, the stator synchronous speed (expressed as letter n_1) should be constant.

The following expression can be obtained from the principle of Figure 1 and formula (1):

$$\begin{aligned} n_1 &= n \pm n_2, \\ \text{or } f_1 &= f \pm f_2. \end{aligned} \tag{2}$$

That is, when the rotor speed (expressed as letter n) is not equal to the synchronous speed (expressed as letter n_1) of the stator, the rotor excitation current frequency (expressed as letter f_2, the corresponding rotating magnetic field speed expressed as letter n_2) and the phase sequence of the rotor excitation current can be adjusted to ensure that the stator synchronous speed (expressed as letter n_1) or the corresponding frequency (expressed as letter f_1) is constant. There are three different relationships between the actual speed of the rotor and the synchronous speed of the stator. The three relationships are greater, equal, and smaller. According to these three different speed relations, the marine asynchronous shaft generator will work in three different states. They are supersynchronization, synchronization, and subsynchronization. In this paper, the subsynchronization working state of the marine asynchronous shaft generator is only discussed and analyzed.

2.2. The Modeling Assumptions. Before establishing the mathematical model of the marine asynchronous shaft generator, there are some assumptions as follows [6]:

(1) The stator winding and rotor winding are completely symmetrical, and the space position is 120° to each other. The magnetic motive force is sinusoidally distributed along the air gap circumference, and the harmonics are ignored.

(2) The saturation effect of the magnetic path is to be ignored. The mutual inductance and self-inductance of windings are assumed to be linear.

(3) The influence of frequency and temperature on the resistance of stator winding and rotor winding will be ignored.

(4) The hysteresis loss and eddy current loss will be ignored.

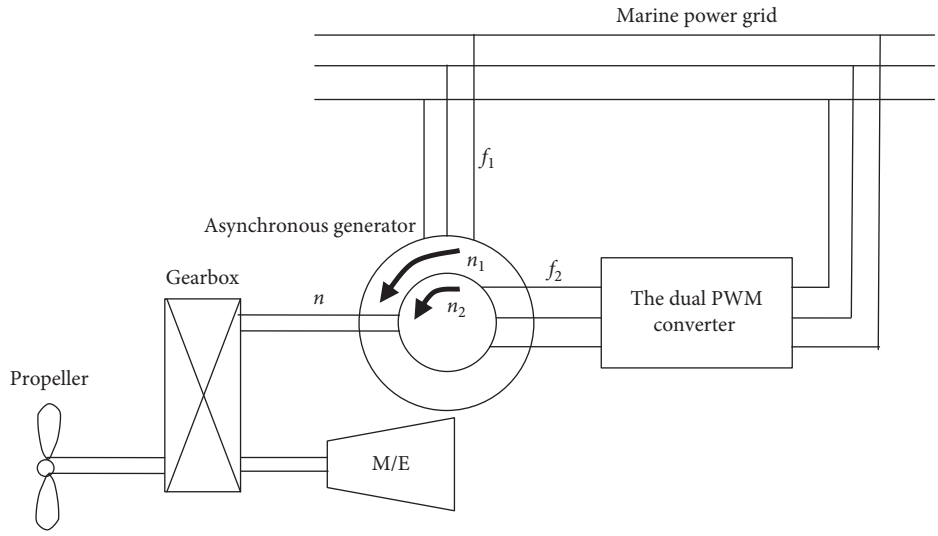

Figure 1: The structure of the marine asynchronous shaft generator system.

(5) The friction and power consumption between propeller main shaft and gearbox will not be considered; the friction and power consumption between gearbox and rotor will not be considered yet.

(6) The motor convention will be adopted on the direction of various physical quantities, including current, voltage, and the flux linkage of stator and rotor.

2.3. Mathematical Model

2.3.1. The Mathematical Model in d-q Coordinate System

(1) The Expression of Energy Balance. It can be seen from Figure 1 that the energy absorption of the marine asynchronous shaft generator consists of two parts. One part of the energy comes from the main engine of the ship, which is represented by the letter P_{SG}. The other part comes from the power converter, which is represented by the letter P_C. Two parts of energy are transferred to the ship power grid through the marine asynchronous shaft generator. In the case of ignoring the loss of the ship power grid, the total output power of the marine asynchronous shaft generator is equal to the total power consumed by all loads in the ship power grid [7, 8]. The energy balance equation of the system is as follows:

$$\begin{aligned} P_M &= P_P + P_{SG}, \\ (P_L)_{SG} &= (P_{SG} + P_C) \times \eta_{SG} = \sum_{i=1}^{n} P_i. \end{aligned} \tag{3}$$

In the energy balance equation shown as formula (3), the letter P_M is used to represent the power output of the main engine of the ship; the letter P_P stands for the power absorbed by the ship's propeller; the letter P_{SG} is used to represent the power transmitted by the main engine to shaft generator through gearbox; the letter $(P_L)_{SG}$ stands for the total power delivered by the marine asynchronous shaft generator to the ship's power grid; the letter P_C represents the electric power supplied by the dual PWM converter to rotor side of the asynchronous generator; the formula $\sum_{i=1}^{n} P_i$ is used to represent the electric power consumed by all electric loads on the ship under the current navigation conditions; the letter η_{SG} stands for the efficiency of the marine asynchronous shaft generator.

(2) The Expression of Flux Linkage. The flux-linkage expression of stator windings and rotor windings in the *d-q* coordinate system is described as follows:

$$\begin{aligned} \psi_{1d} &= L_1 i_{1d} + L_m i_{2d}, \\ \psi_{1q} &= L_1 i_{1q} + L_m i_{2q}, \\ \psi_{2d} &= L_2 i_{2d} + L_m i_{1d}, \\ \psi_{2q} &= L_2 i_{2q} + L_m i_{1q}. \end{aligned} \tag{4}$$

The footmarks of physical quantities of stator and rotor are represented by 1 and 2, respectively, in expression (4). The letter L represents inductance, so the letter L_1 represents the reactance of stator winding. The letter R represents resistance, so the letter R_1 represents the resistance of stator winding. Other letters have similar physical meanings.

(3) The Expression of Voltage. The voltage expression of stator windings and rotor windings in the *d-q* coordinate system is described as follows:

$$\begin{aligned} u_{1d} &= R_1 i_{1d} + p\psi_{1d} - \omega_1 \psi_{1q}, \\ u_{1q} &= R_1 i_{1q} + p\psi_{1q} + \omega_1 \psi_{1d}, \\ u_{2d} &= R_2 i_{2d} + p\psi_{2d} - \omega_s \psi_{2q}, \\ u_{2q} &= R_2 i_{2q} + p\psi_{2q} + \omega_s \psi_{2d}. \end{aligned} \tag{5}$$

In formula (5), the formula described as $\omega_s = \omega_1 - \omega_2$ is used to represent the slip electric angular velocity; the letter D stands for the differential operator.

Combiningg formula (4) and formula (5), the voltage expression can be rewritten as follows:

$$\begin{aligned} u_{1d} &= R_1 i_{1d} + \left(L_1 p i_{1d} + L_m p i_{2d}\right) - \omega_1 \left(L_1 i_{1q} + L_m i_{2q}\right), \\ u_{1q} &= R_1 i_{1q} + \left(L_1 p i_{1q} + L_m p i_{2q}\right) + \omega_1 \left(L_1 i_{1d} + L_m i_{2d}\right), \\ u_{2d} &= R_2 i_{2d} + \left(L_2 p i_{2d} + L_m p i_{1d}\right) - \omega_s \left(L_2 i_{2q} + L_m i_{1q}\right), \\ u_{2q} &= R_2 i_{2q} + \left(L_2 p i_{2q} + L_m p i_{1q}\right) + \omega_s \left(L_2 i_{2d} + L_m i_{1d}\right). \end{aligned} \tag{6}$$

(4) The Expression of Stator Power. The expression of stator active power and stator reactive power can be described as the following formula:

$$\begin{aligned} P_1 &= \frac{3}{2}\left(u_{1d} i_{1d} + u_{1q} i_{1q}\right), \\ Q_1 &= \frac{3}{2}\left(u_{1q} i_{1d} - u_{1d} i_{1q}\right). \end{aligned} \tag{7}$$

It can be seen from expression (7) and formula (6) that the voltage component and current component on the *d-q* axis are coupled and need to be decoupled.

2.3.2. The Mathematical Model in M-T Coordinate System. According to the power expression shown as formula (7), the active power and reactive power of the stator are determined by the voltage and current components on the *d-q* axis. As long as the voltage and current of the *d-q* axis can be controlled independently, the decoupling of active power and reactive power can be realized. In order to realize decoupling, the above mathematical model should be rewritten with stator flux orientation in *M-T* coordinate system. The vector relationship between various parameters of stator and rotor in different coordinate systems is shown in Figure 2.

According to the relationship between the parameters in Figure 2, the power expression (7) can be rewritten in *M-T* coordinate system as formula (8) and the relationship between the components of stator current and rotor current on the T-axis can be described as expression (9).

$$\begin{aligned} P_1 &= \frac{3}{2}\left(u_{M1} i_{M1} + u_{T1} i_{T1}\right), \\ Q_1 &= \frac{3}{2}\left(u_{M1} i_{T1} - u_{T1} i_{M1}\right), \end{aligned} \tag{8}$$

$$\begin{aligned} i_{T1} + i_{T2} &= -i_{d1}\sin\delta + i_{q1}\cos\delta - i_{d2}\sin\delta + i_{q2}\cos\delta \\ &= \left(i_{q1} + i_{q2}\right)\sin\delta - \left(i_{d1} + i_{d2}\right)\sin\delta \\ &= \left[\left(\frac{\psi_0}{L_M}\right)\sin\delta\right]\cos\delta - \left[\left(\frac{\psi_0}{L_M}\right)\cos\delta\right]\sin\delta = 0. \end{aligned} \tag{9}$$

In equation (9), the letter ψ_0 represents the flux linkage, shown as follows:

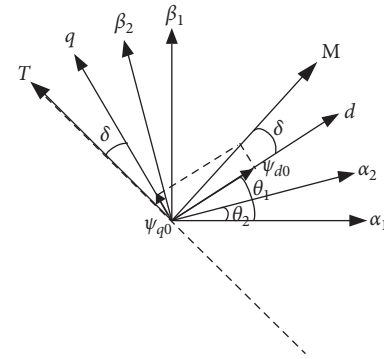

Figure 2: Vector diagram in the *M-T* frame.

$$\psi_0 = L_m\left(i_{M1} + i_{M2}\right). \tag{10}$$

A conclusion can be drawn from equation (9) that the sum of the two current components is equal to zero, described as follows:

$$i_{T1} = -i_{T2}. \tag{11}$$

If the flux linkage of the stator is oriented to the *M*-axis, the flux linkage (expressed as the letter ψ_0) and the component of stator voltage on *T*-axis will be constant; the component of stator voltage on *M*-axis is zero, which can be described as follows:

$$\begin{aligned} u_{M1} &= 0, \\ u_{T1} &= u_1. \end{aligned} \tag{12}$$

According to formula (9), formula (10), formula (11), and formula (12), the active power and the reactive power of stator shown as equation (8) can be rewritten as follows:

$$\begin{aligned} P_1 &= \frac{3}{2}\left(u_{M1} i_{M1} + u_{T1} i_{T1}\right) \\ &= \frac{3}{2}\left[-u_{M1} i_{M2} + \left(\frac{\psi_0}{L_m}\right)\cdot u_{M1} - u_{T1} i_{T2}\right] \approx \frac{3}{2} u_{T1} i_{T1} \\ &= -\frac{3}{2} u_{T1} i_{T2}, \end{aligned} \tag{13}$$

$$\begin{aligned} Q_1 &= \frac{3}{2}\left(u_{M1} i_{T1} - u_{T1} i_{M1}\right) = \frac{3}{2} u_{T1} i_{M1} \\ &= \frac{3}{2}\left[-u_{M1} i_{T2} - \left(\frac{\psi_0}{L_m}\right)\cdot u_{T1} + u_{T1} i_{M2}\right] \\ &\approx \frac{3}{2}\left[u_{T1} i_{M2} - \left(\frac{\psi_0}{L_m}\right)\cdot u_{T1}\right]. \end{aligned} \tag{14}$$

It can be seen from equation (13) that the stator active power (expressed as letter P_1) is proportional to the stator voltage component on the *T*-axis (expressed as the letter u_{T1}) and the rotor current component on the *T*-axis (expressed as the letter i_{T2}). And it can be seen from equation (14) that the stator reactive power Q_1 is related to three physical quantities which includes the stator voltage

component on the T-axis (expressed as the letter u_{T1}), the rotor current component on the M-axis (expressed as the letter u_{T1}), and the constant described as (ψ_0/L_m).

In order to realize decoupling, based on expression (13), the active-power control is taken as the outer control loop of the rotor current component on the M-axis, and the reactive power control is used as the outer control loop of the rotor current component on the T-axis. In other words, the output signal generated by the power controller is used as the given signal of rotor current control.

In this paper, the component of rotor input current on the M-axis and T-axis, represented by i_{M2} and i_{T2}, is used to control the output current of the stator side, denoted by i_{M1} and i_{T1}, respectively. Combined with literature 9 [9], IP control is adopted. In order to make the expression more concise, let $y_1 = i_{M1}$, $y_2 = i_{T1}$, $x_1 = i_{M2}$ and $x_2 = i_{T2}$. The following formula can be obtained according to expression (5):

$$\dot{y}_1 = \frac{L_2R_1}{L_m^2 - L_1L_2}y_1 + \frac{\omega_s L_m^2 - \omega_1 L_2L_2}{L_m^2 - L_1L_2}y_2 - \frac{L_mR_2}{L_m^2 - L_1L_2}x_1 - \frac{(\omega_1 - \omega_s)L_2L_m}{L_m^2 - L_1L_2}x_2 + \frac{L_mu_{M2} - L_2u_{M1}}{L_m^2 - L_1L_2}, \tag{15}$$

$$\dot{y}_2 = -\frac{\omega_s L_m^2 - \omega_1 L_2L_1}{L_m^2 - L_1L_2}y_1 + \frac{L_2R_1}{L_m^2 - L_1L_2}y_2 + \frac{(\omega_1 - \omega_s)L_2L_m}{L_m^2 - L_1L_2}x_1 - \frac{L_mR_2}{L_m^2 - L_1L_2}x_2 + \frac{L_mu_{T2} - L_2u_{T1}}{L_m^2 - L_1L_2}, \tag{16}$$

$$\dot{x}_1 = -\frac{L_mR_1}{L_m^2 - L_1L_2}y_1 + \frac{\omega_1 L_1L_m}{L_m^2 - L_1L_2}y_2 + \frac{L_1R_2 - \omega_s L_1L_m}{L_m^2 - L_1L_2}x_1 + \frac{\omega_1 L_m^2 - \omega_s L_1L_2}{L_m^2 - L_1L_2}x_2 + \frac{L_mu_{M1} - L_1u_{M2}}{L_m^2 - L_1L_2}, \tag{17}$$

$$\dot{x}_2 = -\frac{(\omega_1 - \omega_s)L_1L_m}{L_m^2 - L_1L_2}y_1 - \frac{L_mR_1}{L_m^2 - L_1L_2}y_2 - \frac{\omega_1 L_m^2 - \omega_s L_1L_2}{L_m^2 - L_1L_2}x_1 + \frac{L_1R_2}{L_m^2 - L_1L_2}x_2 + \frac{L_mu_{T1} - L_1u_{T2}}{L_m^2 - L_1L_2}. \tag{18}$$

From formula (15) to (18), there are four unknowns and four equations [10, 11]. After solving the four unknowns, they are carried into formula (13) and formula (14). According to formula (12), the decoupling expression of stator power can be obtained, shown as follows:

$$P = -\frac{3}{2}u_{T1}x_2 = -\frac{3}{2}ui_{T2},$$

$$Q = \frac{3}{2}\left[u_{T1}x_1 - \left(\frac{\psi_0}{L_m}\right)\cdot u_{T1}\right] = \frac{3}{2}\left[ui_{M2} - \left(\frac{\psi_0}{L_m}\right)\cdot u\right]. \tag{19}$$

3. Simulation

According to the above mathematical model, described as formula (9) to formula (16), the change process of torque, speed, current, voltage, reactive power, and active power of the marine asynchronous shaft generator in subsynchronous state is obtained by using simulation software named Matlab/Simulink.

3.1. System Simulation Module. According to the working mechanism of the marine asynchronous shaft generator, the functional characteristics of the rotor side converter and network side converter, the system part simulation module as shown in Figure 3 is built in Simulink environment.

In the simulation, the value of DC bus voltage (represented by the letter U_{DC}) is 460 V. The line voltage of the ship power grid is set at 190 V, and the transformation ratio of the transformer is 380/190. The three-phase symmetrical pure resistance load ($R = 50\,\Omega$) is star connected. Assuming that the speed of the ship's main engine is constant, the torque to the marine asynchronous shaft generator is 5 N·m, which makes it work in subsynchronous state. The parameters of the marine asynchronous shaft generator are shown in Table 1.

3.2. Simulation Waveform

3.2.1. Rotor Speed. When the ship sails stably at full speed on the sea, it is sent to the marine asynchronous shaft generator with constant torque.

The marine asynchronous shaft generator will start under this drive-torque, and the rotor speed will gradually increase and reach a stable state. The corresponding speed waveform is shown in Figure 4.

In Figure 4, after about 1.6 s, the rotor speed can be basically stable, about 1340 r/min, which is lower than the synchronous speed (represented by the letter n_1). The synchronous speed is 1500 r/min, because the pole-airs (represented by the letter p) are two, shown in Table 1. The marine asynchronous shaft generator will work in a subsynchronous state.

3.2.2. The Torque Waveform. When the ship sails steadily at full speed on the sea, the torque transmitted to the marine asynchronous shaft generator will be constant, and the corresponding electromagnetic torque change process of the marine asynchronous shaft generator is shown in Figure 5.

When time (represented by the letter t) is at zero, the marine asynchronous shaft generator is started by the main

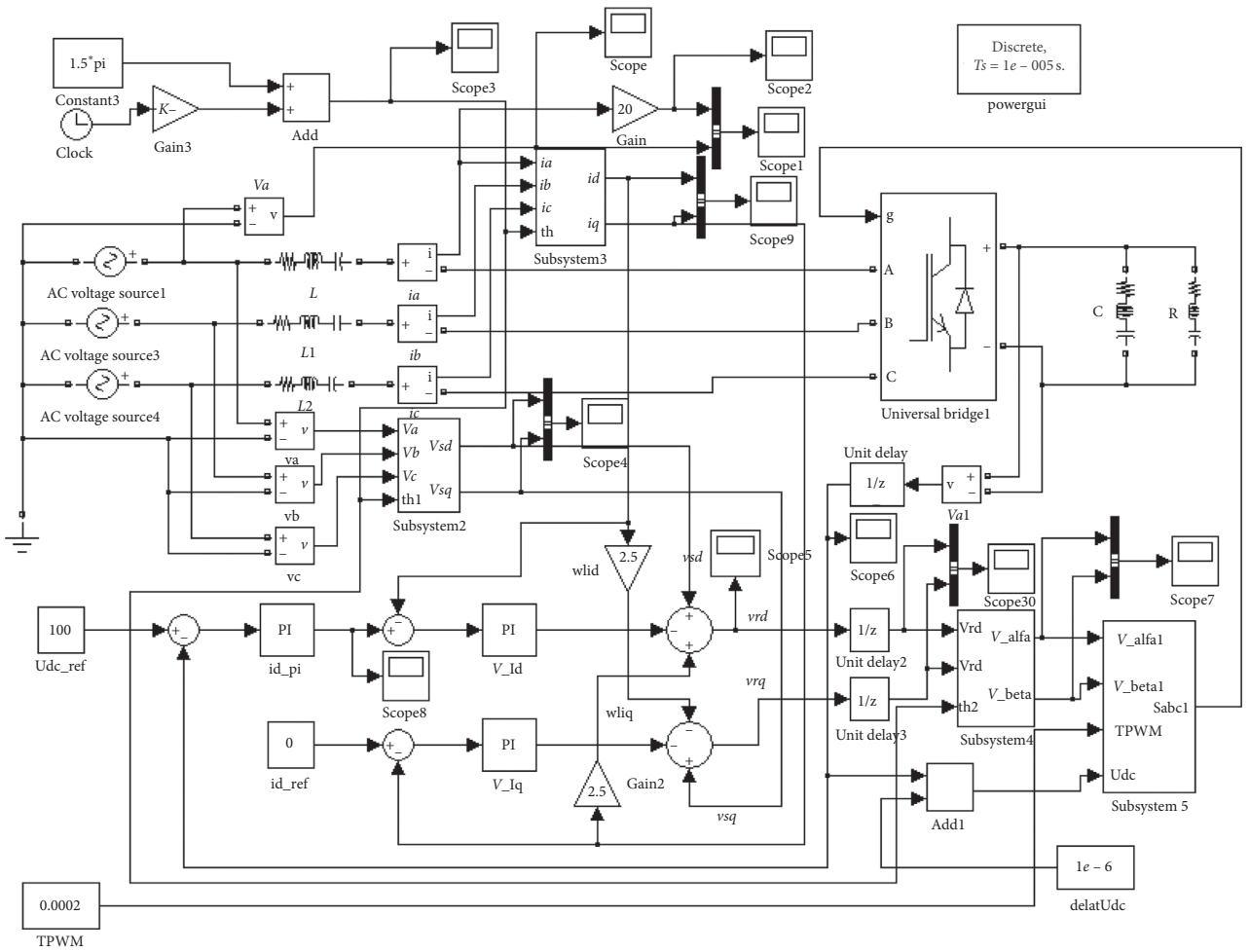

Figure 3: Simulation module of subsynchronization.

Table 1: Parameters of the marine asynchronous shaft generator.

Name	Value
U_e (V)	380
P_e (kW)	6
f_1 (Hz)	50
P	2
J (kg·m^2)	0.05
R_1 (Ω)	1.37
L_1 (H)	0.1613
R_2 (Ω)	1.65
L_2 (H)	0.9955
L_{12} (H)	0.1588

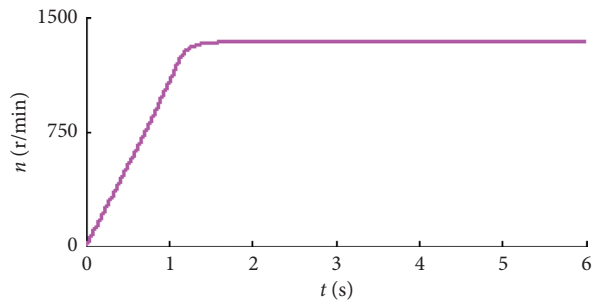

Figure 4: Rotor speed at subsynchronization.

engine driving torque. During the starting period of 0–1.6 s, the torque waveform changes greatly. After 1.6 s of stability, the electromagnetic torque is about −5 N·m. The electromagnetic torque is negative, which means the direction of electromagnetic torque is opposite to that of the rotor speed.

3.2.3. The Line Voltage of Rotor Side Converter. The line voltage between phase A and phase B of the rotor side converter is shown in Figure 6, which is about 460 V and basically stable, and will provide excitation for the rotor. The voltage value shown in Figure 6 is consistent with the voltage setting value of 460 V of the double PWM intermediate DC bus. It can be seen from Figure 6 that the voltage frequency is relatively high before 1.6 seconds in the starting stage of the marine asynchronous shaft generator, and after 1.6 seconds, the frequency becomes lower and almost unchanged. The voltage waveform tends to be stable. And the marine asynchronous shaft generator is in a stable subsynchronous state.

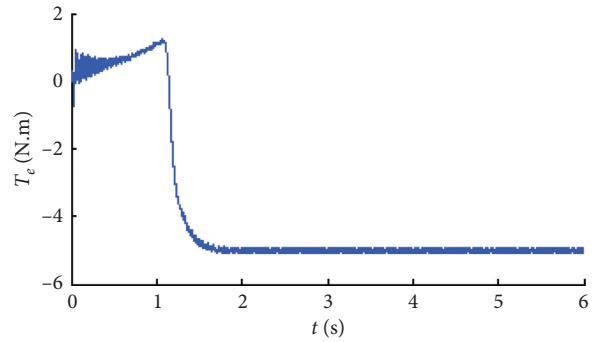

Figure 5: The electromagnetic torque.

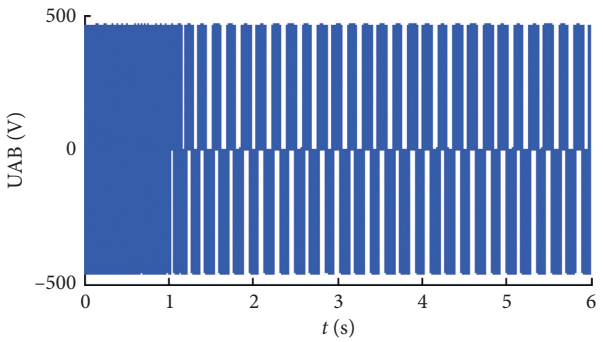

Figure 6: Output line voltage of the rotor side converter.

3.2.4. The Voltage Component and Current Component of Rotor on d-Axis and q-Axis. The components of rotor voltage and rotor current on the d-axis and q-axis are shown in Figures 7 and 8, which tend to be stable at about 1.6 seconds. The unstable state before 1.6 seconds is defined as the starting process of the marine asynchronous shaft generator.

It can be seen from Figures 7 and 8 that the components of rotor voltage and rotor current on the d-axis and q-axis are constant after stability, without alternating, and the frequency is zero.

3.2.5. Three-Phase Current of Rotor. The Rotor current waveform of phase A is shown in Figure 9(a), and the rotor current waveform of phase ABC is shown in Figure 9(b). The marine asynchronous shaft generator enters the stable state about 1.6 seconds after starting, and the magnitude and frequency of rotor excitation current remain unchanged after stability.

3.2.6. Active Power and Reactive Power. The simulation waveforms of active power and reactive power in the sub-synchronous state are shown in Figure 10. The negative sign shown in Figure 10 means the power of the generator is output. The reactive power and active power are stable after 1.6 seconds, and the reactive power (represented by the letter Q_1) is about zero after stabilization, the active power (represented by the letter P_1) is approximately constant.

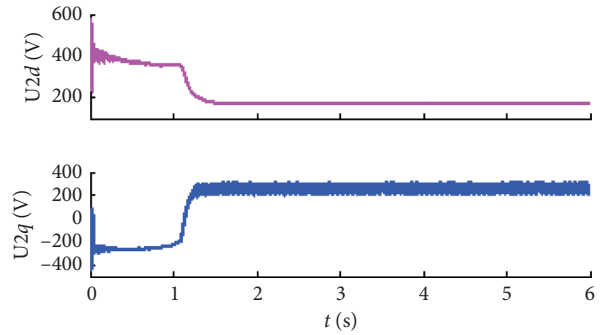

Figure 7: Component of rotor voltage on the d-axis and q-axis.

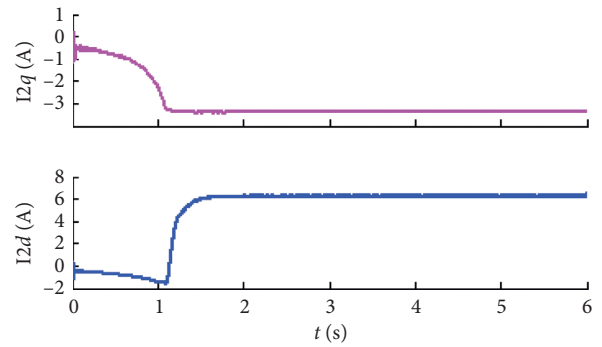

Figure 8: Component of rotor current on the d-axis and q-axis.

3.2.7. Stator Voltage and Stator Current. In order to display the changing trend of stator phase A current and phase A voltage in the same coordinate, the current is amplified by −10 times. The magnification is negative because the motor convention is used in the modeling process; the phase of voltage and current is opposite. Otherwise, because the current value is too small, the changing trend of current cannot be clearly seen in the same coordinate system with voltage. The simulation waveform of the stator voltage waveform and stator current is shown in Figure 11(a), with the negative ten times current waveform.

It can be read from Figure 11(a) that the period of stator A-phase voltage and A-phase current is 0.02 s. That is, the frequency is 50 Hz. Since the given load is pure resistive load, the voltage and current in the simulation results are in the same frequency and phase, and the actual current waveform of stator A-phase is shown in Figure 11(b).

3.3. Result Analysis of Simulation Waveform. The voltage and current of stator A-phase in Figure 11(a) are in the same frequency and phase. It can be deduced that the reactive power is zero, which is consistent with the simulation waveform of zero reactive power described in Figure 10 and consistent with the simulation premise that the load is pure resistance load.

The stator phase A current (the peak-value is about 3 A) is shown in Figure 11(b), and the stator voltage (the peak-value is about 160 V) is shown in Figure 11(a), and the corresponding power including the active power and reactive power can be calculated; the power factor also can be

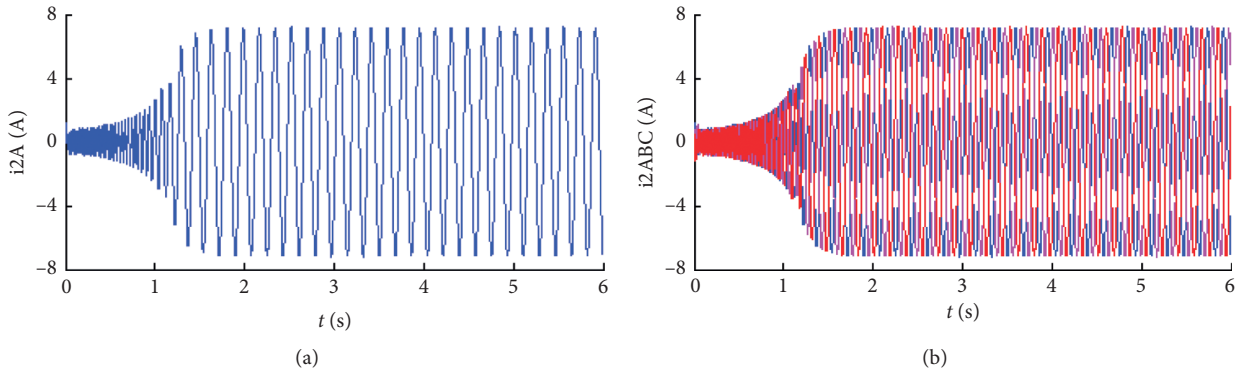

Figure 9: Rotor current in the subsynchronous state. (a) Phase A. (b) Phase ABC.

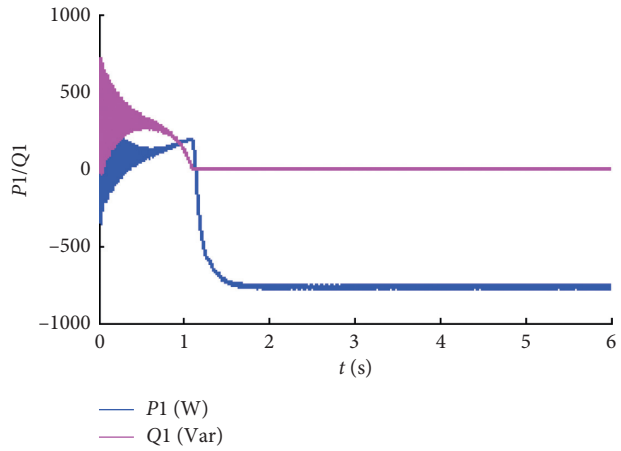

Figure 10: Active power and reactive power.

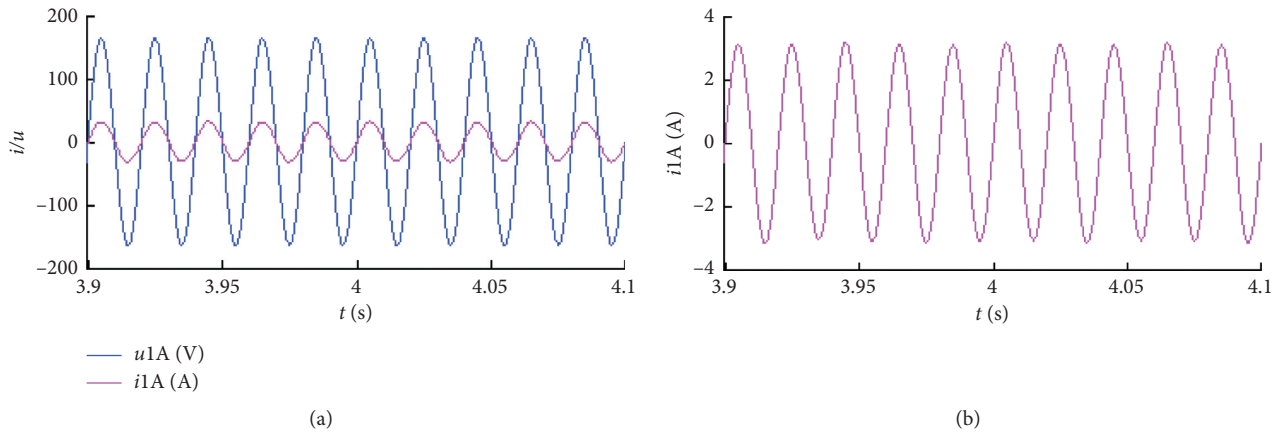

Figure 11: Stator voltage and stator current in subsynchronous state. (a) Voltage and current (–10 times). (b) Actual stator current.

calculated. The active power is calculated to be about 720 W, and the reactive power is zero, the corresponding power factor is 1. The calculated results are consistent with the simulation waveforms described in Figure 10.

According to the calculated active power of 720 W and the speed of 1340 r/min described in Figure 4, the corresponding torque can be calculated under the premise of modeling, which is about 5 N·m. The torque calculation results are consistent with the electromagnetic simulation waveform shown in Figure 6.

According to the speed waveform of 1340 r/min shown in Figure 4, the corresponding frequency of rotor speed can

be calculated, which is about 44.7 Hz. The sum of this frequency with a value of 44.7 Hz and the rotor excitation current frequency is shown in Figure 9 (about 5.5 Hz) is 50.17 Hz, which is basically consistent with the corresponding frequency (50 Hz) of stator synchronous speed because there may be some errors in reading the pictures.

4. Experiment

4.1. Overview of Experimental Platform. The hardware part of the marine asynchronous shaft generator experimental platform in the laboratory mainly includes the main circuit and control circuit, which is mainly composed of variable frequency motor used to simulate the main engine of a ship, asynchronous generator, transformer, frequency converter, back-to-back dual PWM converter, reactors, and grid-connected relay. The schematic diagram is shown in Figure 12.

In Figure 12, the city power on the laboratory wall is used to simulate the 380 V ship power grid. The frequency converter drives the variable frequency motor to simulate the main engine of the ship. Different frequencies are set to simulate the speed of the main engine under different working conditions. The variable frequency motor drives the asynchronous generator to generate electricity. The above equipment together constitutes the marine asynchronous shaft generator experimental platform. The stator output voltage of the doubly fed shaft generator can be connected to the power grid of the ship through the main switch shown in Figure 12 after the transformer step-down. The transformation ratio of the three-phase transformer is 2 (380/190). At the same time, the voltage is sent to the rectifier stage of the dual PWM converter. And the inverter stage of the dual PWM converter outputs sinusoidal AC to the rotor of the doubly fed shaft generator for excitation.

The hardware layout of the experimental platform is shown in Figure 13. The power of the frequency converter, variable frequency motor, and the asynchronous generator is 3.7 kW, 7.5 kW, and 6 kW, respectively, and the pole pairs of the variable frequency motor and the doubly fed generator are both 2. The maximum speed of the variable frequency motor and the doubly fed generator is 1800 r/min.

4.2. The Experimental Results. In the experiment, the grid side converter is powered on and the input voltage is 190 V. The voltage with 190 V is obtained by reducing the voltage of 380 V through a transformer, with a transformation ratio of 2, as shown in Figure 12. The dual PWM converter is put into operation for rectification. The voltage on the intermediate DC bus will increase gradually and finally stabilizes at 460 V, which is prepared for rotor excitation.

The speed of the simulated main engine is set by frequency conversion, and at the same time, the rotor of the asynchronous generator is driven to rotate. The frequency of the frequency converter is changed to realize the speed change of the marine main engine simulated by the variable frequency motor. The rotor speed is stable at 1340 r/min by changing the frequency of the frequency converter. The marine asynchronous shaft generator will work in subsynchronous state. The load in the experiment is a three-phase symmetrical pure resistance load (represented by the letter R_L, $R_L = 50\,\Omega$), and star connected.

The waveforms of the experimental results are shown in Figures 14– 16.

4.2.1. The Waveform of DC Bus Voltage. The stable DC bus voltage waveform is shown in Figure 14, and it is 460 V after stabilization, which lays the foundation for providing a suitable rotor excitation current. The experimental waveform is consistent with the 460 V of simulation waveform shown in Figure 6.

4.2.2. Rotor Excitation Current Waveform in Subsynchronous State. The experimental waveform of the three-phase current of rotor winding during subsynchronous stable operation is shown in Figure 15.

The period of rotor excitation current under subsynchronous stable state can be read out from Figure 15 as follows:

$$T \approx \frac{30\,\text{ms}}{\text{grid}} \times 6\,\text{grid} = 180\,\text{ms} = 0.18\,\text{s}. \tag{20}$$

From formula (20), the period (represented by the letter T) of rotor excitation current is 0.18 seconds. It can be calculated that the rotor excitation current frequency (represented by the letter f_2) is as follows:

$$f_2 = \frac{1}{T} = \frac{1}{0.18} \approx 5.55. \tag{21}$$

Because of the existence of error in reading graphs, the calculated frequency described as formula (21) is basically consistent with the slip frequency corresponding to the rotor speed of 1340 r/min. And the slip frequency is represented by the letter f_s, shown in the following formula:

$$f_s = \frac{\Delta n \times p}{60} = \frac{(1500 - 1340) \times 2}{60} \approx 5.33. \tag{22}$$

4.2.3. Stator Voltage and Stator Current. The voltage and current of stator phase A are shown in Figure 16.

In order to be able to see the changing trend and phase relationship of voltage and current in the same coordinate system, the output waveform of experimental current shown in Figure 16 was amplified by 4 times of actual current. It can be seen from Figure 16 that the stator voltage and current are sinusoidal AC with the same period and same frequency, the amplitude of the voltage is 160 V, and the amplitude of the current is about 3 A. The period (represented by the letter T) can be calculated as follows:

$$T = \frac{10\,\text{ms}}{\text{grid}} \times 2\,\text{grid} = 20\,\text{ms} = 0.02\,\text{s}. \tag{23}$$

The phase between the stator current of phase A and the stator voltage of phase A is the opposite. The reason is that the current direction in the experimental measurement is

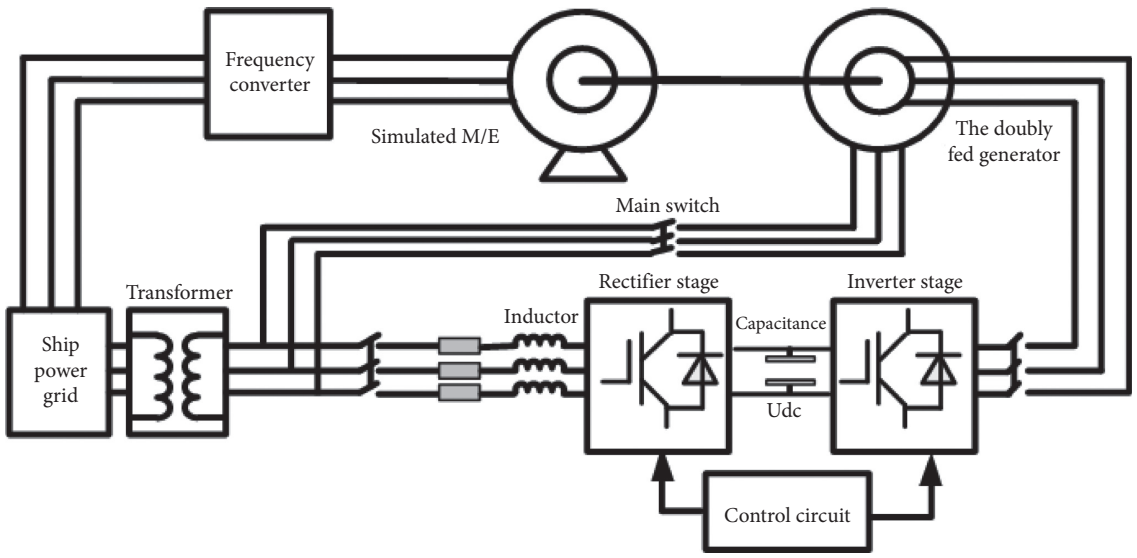

Figure 12: Schematic diagram of the experimental platform.

(a) (b) (c)

Figure 13: Experimental platform photos. (a) Prime mover and generator. (b) Transformer and reactor. (c) The dual PWM converter.

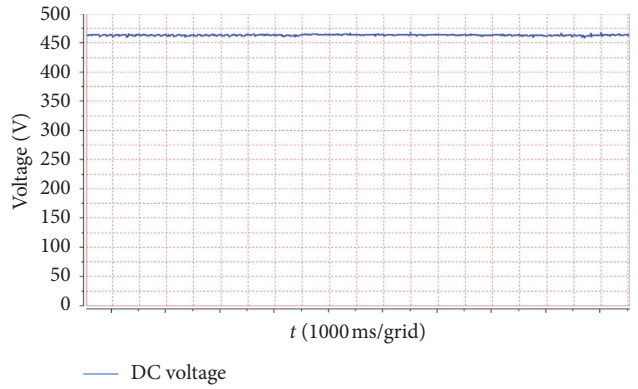

Figure 14: DC bus voltage 460 V.

opposite to the actual current direction of the generator. The actual current waveform direction is the reverse of the current waveform in Figure 16. The phase difference is 180°, as is shown in Figure 16. Therefore, in Figure 16, the variation trend of stator output voltage and stator current is consistent with that of the simulation waveform shown in Figure 11.

4.3. Summary. The following conclusions can be drawn from the comparison between the simulation waveform and the experimental waveform:

(1) The value, frequency, and changing trend of stator and rotor parameters in the simulation diagram are consistent with the experimental results.

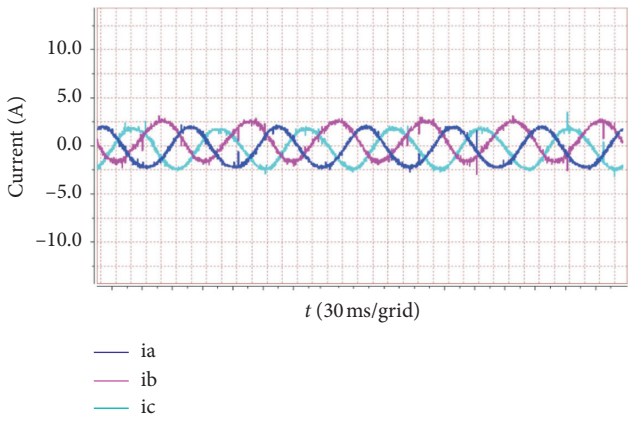

Figure 15: Rotor current in subsynchronous stable operation.

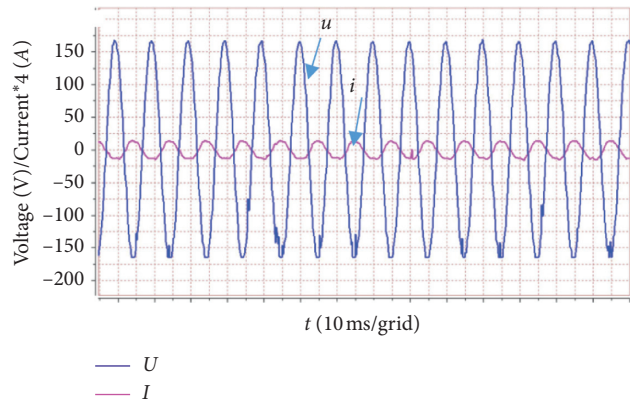

Figure 16: Stator voltage and stator current.

(2) Because the influence of temperature, frequency, and other physical parameters on the stator and rotor winding resistance is ignored in the modeling process, the simulation waveform results are generally smoother than the experimental waveform, and the harmonics are less.

(3) The above simulation results are in good agreement with the actual situation, which proves the correctness of the mathematical model, which is helpful to the development of the marine asynchronous shaft generator simulator.

5. Conclusion

In this paper, the modeling and subsynchronous simulation of a new marine asynchronous shaft generator are carried out. The relationship between the physical quantities in the simulation waveform is consistent with the actual situation, which is verified by experiments. The consistency of simulation results and experimental waveforms proves the correctness of the mathematical model. It lays a theoretical foundation for the development of a virtual simulation system and fault diagnosis system of the marine asynchronous shaft generator, which is helpful for crew training.

Data Availability

All data generated or analyzed during this study are included in this article.

Conflicts of Interest

The authors declare that they have no conflicts of interest.

References

[1] R. Zhu, Z. Chen, Y. Tang, F. Deng, and X. Wu, "Dual-loop control strategy for DFIG-based wind turbines under grid voltage disturbances," *IEEE Transactions on Power Electronics*, vol. 31, no. 3, pp. 2239–2253, 2016.

[2] S. Lekhchine, T. Bahi, I. Abadlia, Z. Layate, and H. Bouzeria, "Speed control of doubly fed induction motor," *Energy Procedia*, vol. 74, no. 74, pp. 575–586, 2015.

[3] T.-K. T. Layate, N.-V. Nguyen, An efficient four-state zero common-mode voltage PWM scheme with reduced current distortion for a three-level inverter," *IEEE Transactions on Industrial Electronics*, vol. 65, no. 2, pp. 1021–1030, 2018.

[4] F. Xiong, X.-f. Wang, and B. Hua, "D-q axis mathematical model of wound-rotor brushless doubly-fed machine," *Electric Machines and Control*, vol. 19, no. 5, pp. 81–88, 2015.

[5] P. Ma, W. Liu, and S. Mao, "Dead-time compensation method of single-phase AC excitation for three-stage brushless synchronous machines," *Zhongnan Daxue Xuebao (Ziran Kexue Ban)*, vol. 47, no. 12, pp. 4048–4055, 2016.

[6] K. Yu and P. Tang, "Equivalent circuit model and characteristic analysis of brushless douly-fed machine," *Proceeding of the CSEE*, vol. 38, no. 14, pp. 4222–4232, 2018.

[7] G. Liu, X. Wang, and F. Xiong, "A "Π" –type equivalent circuit of wound rotor brushless doubly-fed machines," *Proceedings of the CSEE*, vol. 36, no. 20, pp. 5632–5639, 2016.

[8] T. Trivedi, R. Jadeja, and P. Bhatt, "Improved direct power control of shunt active power filter with minimum reactive power variation and minimum apparent power variation approaches," *Journal of Electrical Engineering and Technology*, vol. 12, no. 3, pp. 1124–1136, 2017.

[9] Y. Lang-tao, D. Wang, and S.-l. Wang, "Modeling and simulation of DFIG decoupling control based on IP control," *Power System Protection and Control*, vol. 40, no. 20, pp. 113–118, 2012.

[10] S.-H. Gan, S.-M. Bi, W. Gu, and C. Jian-xin, "Improved Z-source grid-connected inverter of ship shaft generator," *Dianji Yu Kongzhi Xuebao*, vol. 22, no. 12, pp. 68–76, 2018.

[11] D. Liang, D. Wang, and Z. Peng, "Synchronization of ship shaft DFIG based on linear active disturbance rejection control," *Small & Special Electrical Machines*, vol. 45, no. 2, pp. 83–87, 2017.